ChemPubSoc Europe

DOI: 10.1002/chem.201301679

CHEMISTRY A European Journal Full Paper

Micellar Catalysis

Transfer Hydrogenation of Ketones Catalyzed by Surface-Active Ruthenium and Rhodium Complexes in Water

Alexander M. Kalsin,*[a, b] Tat'yana A. Peganova,[a] Valentin V. Novikov,[a] Alexandra I. Zhamoytina,[c] Luca Gonsalvi,*[b] and Maurizio Peruzzini*[b]

Abstract: An improved, high-yield, one-pot synthetic procedure for water-soluble ligands functionalized with trialkyl ammonium side groups $H_2N(CH_2)_2NHSO_2$-*p*-$C_6H_4CH_2[NMe_2(C_nH_{2n+1})]^+$ ($[\mathbf{HL}^n]^+$; $n=8$, 16) was developed. The corresponding new surface-active complexes [(*p*-cymene)RuCl($\mathbf{L}^n$)] and [Cp*RhCl($\mathbf{L}^n$)] (Cp* = η^5-C_5Me_5) were prepared and characterized. For $n=16$ micelles are formed in water at concentrations as low as 0.6 mM, as demonstrated by surface-tension measurements. The complexes were used for catalytic transfer hydrogenation of ketones with formate in water. Highly active catalyst systems were obtained in the case of complexes bearing C_{16} tails due to their ability to be adsorbed at the water/substrate interface. The scope of these catalyst systems in aqueous solutions was extended from partially water soluble aryl alkyl ketones (acetophenone, butyrophenone) to hydrophobic dialkyl ketones (2-dodecanone).

Introduction

Over the last 20 years asymmetric transfer hydrogenation (ATH) of ketones has become a versatile and powerful method for the synthesis of enantiomerically pure secondary alcohols, especially with efficient catalysts such as [(η^6-arene)RuCl(TsDPEN)][1] and [Cp*MCl(TsDPEN)] (M = Rh, Ir;[2] Cp* = η^5-C_5Me_5; TsDPEN = 2-amino-1,2-diphenylethyl(*p*-tosyl)amide). Aldehydes[3] and imines[4] were also reduced by this method. The reaction can tolerate conjugated double[5] and triple[6] bonds or α-halogenated substituents,[7] but sometimes hydrogenation of a conjugated C=C bond can occur instead of the desired reduction of a carbonyl group.[8] In 2001 the first case of transfer hydrogenation of ketones with HCOONa in aqueous solution catalyzed by Ru^{II} proline complexes was reported.[9] Since then several reviews have been published by Xiao et al. on transfer hydrogenation in aqueous solution.[10] Different approaches using water-soluble ligands and catalysts have been investigated; in particular, aryl-sulfonated[7a,11] and polyethylene-glycol-supported[12] TsDPEN-type ligands functionalized with heterocyclic[13] or trialkyl ammonium[13c,14] groups have been synthesized. In some cases polymer-supported[15] or chitosan-anchored[16] catalysts have been used, but the unmodified TsDPEN-based catalysts sometimes performed better.[3,17] Surfactants have been shown to have generally little effect on the reaction,[7b,18] although in specific cases they improved catalytic performance significantly.[19] Solid substrates could also be readily hydrogenated with HCOONa in emulsions prepared by sonication in the presence of a surfactant in water.[20] Only a few examples of surface-active catalysts that can promote aqueous transfer hydrogenation by improving both the catalytic reaction and the mass transfer between the reagents have been described so far. Recently two types of 2-aminoethyl(*p*-tosyl)amide (Ts-EN) ligands with NEt_3, NMe_2Oct and NBu_3 substituents were reported.[14] Transfer hydrogenation of benzaldehyde with HCOONa in water catalyzed by ruthenium and/or iridium complexes prepared in situ from these ligands gave contrasting results depending on the presence and type of substituents, and it was not clear from these examples whether surface-active ligands had generally a positive effect on hydrogenation rate.[14] An amphiphilic-polymer-based iridium catalyst that can assemble at the interface of emulsion droplets showed remarkable rate acceleration in transfer hydrogenation of aldehydes in water,[21] which was attributed to the high surface area of the emulsion droplets formed during the reaction and the high local concentration of reactants around the active sites. Recently, TsDPEN-based chiral surfactant-type ligands have been used in micellar rhodium catalysis, with higher *ee* values in transfer hydrogenation of various aryl alkyl and dialkyl ketones than the

[a] Dr. A. M. Kalsin, Dr. T. A. Peganova, Dr. V. V. Novikov
A.N. Nesmeyanov Institute of Organoelement Compounds (INEOS RAS)
Russian Academy of Sciences
28 Vavilova St., Moscow 119991 (Russia)
Fax: (+7) 4991350176
E-mail: kalsin@ineos.ac.ru

[b] Dr. A. M. Kalsin, Dr. L. Gonsalvi, Dr. M. Peruzzini
Istituto di Chimica dei Composti OrganoMetallici (ICCOM CNR)
Consiglio Nazionale delle Ricerche
Area di Ricerca di Firenze, via Madonna del Piano 10
50019 Sesto Fiorentino (FI) (Italy)
Fax: (+39) 0555225203
E-mail: l.gonsalvi@iccom.cnr.it
maurizio.peruzzini@iccom.cnr.it

[c] A. I. Zhamoytina
Alexandra I. Zhamoytina
Frumkin Institute of Physical Chemistry and Electrochemistry
Russian Academy of Sciences
31 Leninsky Prospect, Moscow 119991 (Russia)

nonmicellar analogues.[22] Nevertheless, the number of reports on surface-active catalysts for transfer hydrogenation is very limited, and many aspects of their interfacial behavior remain unexplored, also due to the lack of a general and convenient method of functionalization of Ts-EN ligands with surface-active groups.

Here we report on the synthesis of surface-active diamine ligands with quaternized ammonium groups $H_2N(CH_2)_2NHSO_2$-*p*-$C_6H_4CH_2[NMe_2(C_nH_{2n+1})]^+$ (**[HL^n]$^+$**, $n=8$, 16) and with an NEt_3 group **[HL^{Et}]Cl·HCl** by a one-pot procedure that is improved compared to the literature method[14b] and gives nearly quantitative yields. These ligands were used to obtain the corresponding novel ruthenium [(*p*-cymene)RuCl(**L^n**)]Cl and rhodium [Cp*RhCl(**L^n**)]Cl complexes **ML^n** ($n=8$, 16), which were then tested in aqueous transfer hydrogenation of hydrophilic and hydrophobic ketones. The effects of the nature of ancillary ligands, micelle formation and different absorption at the water/substrate interface are also discussed.

Results and Discussion

Synthesis of water-soluble ligands and complexes

Recently, the synthesis of monotosylated diamine ligands having an NR_3^+ group (R = NEt_3, NBu_3, Me_2NOct, Py, 3-methylimidazolyl) in the benzylic position of the tosylate group was reported.[14b] In three steps, *N*-*tert*-butoxycarbonylethylenediamine (Boc-En) was converted to the desired hydrochloride salts of the diamine ligand in 50–65% yield. We modified the known procedure leading to ligands of general formula **[HL^n]Cl·HCl** ($n=8$, 16) using a new one-pot high-yielding method (Scheme 1). The first two synthetic steps, that is, sulfonylation and quaternization, were combined by carrying out the synthesis in dichloromethane over a short reaction time at room temperature without the need to isolate the *N*-Boc-*N*′-(4-bromomethyl)benzenesulfonylethylenediamine intermediate. To suppress side amination of the benzylic position using a protecting Boc-En group, we found that a mixture of Boc-En and tertiary amine should be added to a solution of the sulfonyl chloride, instead of using the reversed order of addition reported in the original procedure.[14b] The corresponding benzyl bromide was isolated by extraction with diethyl ether in 92% yield, a significant improvement compared to what was previously obtained (65% yield).[14b] In step b, the reaction mixture was kept at room temperature for only 2–4 h to ensure complete quaternization of the alkyl dimethyl amine. Longer reaction times should be avoided, as side quaternization of excess amine with dichloromethane to give $ClCH_2NMe_2(C_nH_{2n+1})^+Cl^-$ takes place.[23] Before deprotection with concentrated aqueous HCl, the *N*-Boc-substituted ligand was quenched with aqueous $KHCO_3$ and washed with *n*-hexane or diethyl ether to eliminate the trialkyl ammonium salt and free amine. After deprotection, to obtain pure chloride salts and eliminate bromide, which may still be present as counterion (up to 10%), repeated treatment of the crude product with hydrochloric acid and solvent evaporation were required. This method was also used to obtain the known monotosylated diamine ligand bearing a triethylammonium group **[HL^{Et}]Cl·HCl**. The ligands were isolated in nearly quantitative yield (93–97%) as hydrochloride salts.

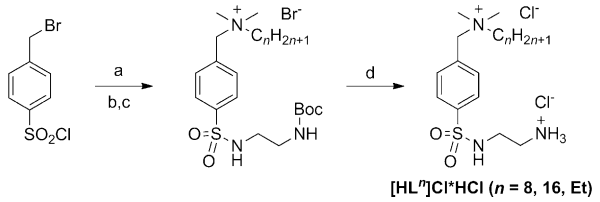

Scheme 1. One-pot synthesis of the ligands **[HL^n]Cl·HCl** ($n=8$, 16). a) *N*-Boc-En/$Me_2NC_nH_{2n+1}$ (1:1), CH_2Cl_2, 0 °C; b) $Me_2NC_nH_{2n+1}$ (1.2 equiv), 25 °C, 4 h; c) $KHCO_3/H_2O$; d) 12 M aqueous HCl.

All ligands were characterized by ^1H and $^{13}C\{^1H\}$ NMR spectroscopy and elemental analysis. As expected, the trialkyl ammonium group imparts water solubility to the ligands, which were then used to obtain the corresponding water-soluble [(*p*-cymene)RuCl(**L^n**)]Cl (**RuL^n**; $n=8$, 16) and [Cp*RhCl(**L^n**)]Cl (**RhL^n**; $n=8$, 16) complexes. The complexes were synthesized in a biphasic water/dichloromethane medium from a suitable organometallic precursor in the presence of potassium bicarbonate and sodium chloride (Scheme 2). NaCl was required to reduce the solubility of the desired complex in the aqueous phase for better extractive workup and to ensure full formation of the chloride derivatives.

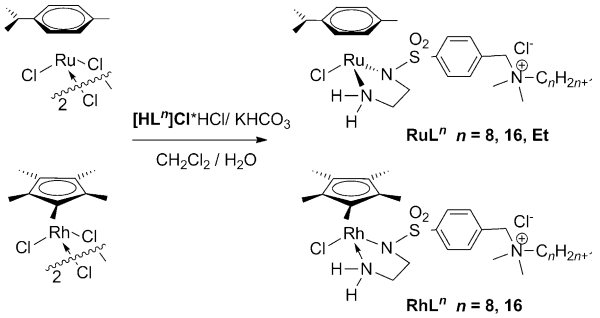

Scheme 2. Synthesis of Ru^{II} and Rh^{III} complexes bearing **[HL^n]Cl*HCl** ($n=8$, 16).

Complexes **RuL^n** and **RhL^n** were characterized by ^1H and $^{13}C\{^1H\}$ NMR spectroscopy, ESI-MS, and elemental analysis. The ^1H NMR spectra of **RuL^n** in $[D_2]$dichloromethane confirmed the formation of the proposed ruthenium arene complexes with three different coligands. All proton resonances of the ethylenediamine moiety, *p*-cymene, the diastereotopic protons of the benzylic CH_2 group, *N*-methyl groups, and methyl groups of the isopropyl group were non-equivalent, as were the ^{13}C NMR resonances of methyl groups in NMe_2 and *p*-cymene. The ^1H NMR spectrum of **RhL^n** in $[D_4]$MeOH was in agreement with the expected C_s-symmetric structure (see Experimental Section). In $[D_2]$dichloromethane the ^1H NMR signals appeared broadened, most likely due to an exchange process in solution. The ESI-MS data were in agreement with the proposed struc-

tures and showed only two groups of peaks at *m/z* values corresponding to the molecular cations [M^+] and [M^+−HCl]. Due to the presence of long alkyl chains, it was not possible to obtain suitable single crystals for collection of X-ray diffraction data.

Micellar properties of ML^n

To determine the surface-active properties and aggregation of complexes **ML^{16}**, translational diffusion coefficients in aqueous solutions were measured by diffusion-ordered NMR spectroscopy (DOSY) at concentrations in the range 0.5–5 mM, the same as that used in the catalytic tests. The effective size of the aggregates in solution was estimated[24] by converting the diffusion coefficients to the corresponding hydrodynamic radii by using the Stokes–Einstein equation or other models.[25] While in the case of micelle formation fast exchange between free monomers and aggregates can lead to underestimation of micelle size,[18] the concentration dependence of the diffusion coefficients allows important micelle characteristics, such as critical micelle concentration (CMC), to be estimated.[26] The diffusion coefficients *D* and calculated hydrodynamic radii r_H for complexes **ML^n** at different concentrations in water are collected in Table 1.

Table 1. Diffusion coefficients and hydrodynamic radii of **ML^n** in water.[a]

Complex	*c* [mM]	10^{11} *D* [$m^2 s^{-1}$]	r_H [nm]
RuL^8	0.5	31.3	0.64
RuL^8	5	33.5	0.60
RhL^8	0.5	41.5	0.48
RhL^8	5	41.4	0.48
RuL^{16}[b]	5	65.7	0.60
RuL^{16}	0.5	14.1	1.41
RuL^{16}	1	9.9	2.01
RuL^{16}	5	6.7	2.97
RhL^{16}	0.5	6.2	3.21
RhL^{16}	5	5.9	3.37

[a] For conditions and details, see Experimental Section. [b] In CD_3OD.

The complexes with shorter alkyl tails **ML^8** showed relatively high diffusion coefficients, with no aggregation in 0.5–5 mM aqueous solutions. The very small r_H values for **RuL^8** in water, which are close to those of **RuL^{16}** in CD_3OD, suggest monomers under these conditions. By increasing the length of the alkyl tail, a dramatic increase of the r_H values for **ML^{16}** was observed, which suggests aggregation and formation of micelles. For complex **RuL^{16}** partial aggregation can occur at concentrations as low as 0.5 mM. At 5 mM concentration, the r_H value was calculated to be 3.0 nm, characteristic of micelles with an aggregation number of about 100 molecules. For **RhL^{16}** little concentration dependence of the *D* value was observed in 0.5–5 mM aqueous solutions, which again suggests aggregation and a CMC of about 0.5 mM or lower. The micelle radii estimated for **RhL^{16}** (3.2–3.4 nm) are slightly larger than those found for 5 mM **RuL^{16}**, likely due to the higher hydrophobicity of the Cp* ligand compared to η^6-*p*-cymene in **RuL^{16}**. In this case less ordered (bulkier) and less hydrated **RhL^{16}** micelles are likely to form. Similarly, the r_H value of **RhL^8** (0.48 nm) estimated from DOSY experiments was smaller than that of **RuL^8** (0.60 nm) due to a lower degree of hydration and more compact folding of **RhL^8**.

The CMCs of **ML^{16}** were confirmed by measuring the surface tension γ of solutions of **RuL^{16}** and **RhL^{16}** as a function of concentration (Figure 1). The minimum in γ corresponds to the

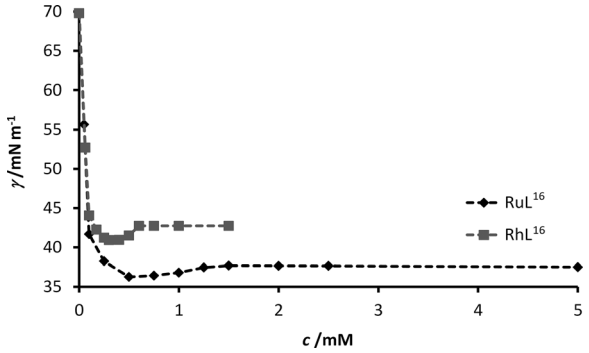

Figure 1. Surface tension γ versus concentration *c* for **ML^{16}** at 25±0.5 °C.

pre-CMC transition (PCT) of **ML^n** in the chosen medium; the post-minimum inflection at maximum γ values corresponds to the CMC.[27] The CMCs determined for **RuL^{16}** and **RhL^{16}** were 1.3 and 0.6 mM, respectively.[28] The CMCs obtained by this technique are in agreement with those previously estimated by DOSY NMR experiments.

Interestingly, the CMC of **RuL^{16}** (ca. 1.3 mM) compares well with that of $C_{16}H_{33}NMe_3^+Cl^-$ (CTAC).[29] In parallel, the r_H value of 2.97 nm approximates well to the size of CTAC micelles (2.43 nm[30]) plus the size of the [(*p*-cymene)Ru(Ts-EN)] organometallic moiety. The micellar behavior of **RuL^{16}** should thus resemble that of CTAC. Unfortunately, it was not possible to obtain a direct measurement of the CMC of **RuL^8**. However, we can assume it to be on the order of that of $C_8H_{17}NMe_3^+Br^-$ (OTAB, CMC = 250 mM[31]), which is much higher than the range of concentrations used in the corresponding catalytic tests. In summary, surface tension measurements and calculations of CMCs prove that **RhL^{16}** is less surface active than **RuL^{16}** and CTAC,[29] and this confirms the above discussed arguments based on DOSY measurements on the different organizations of the micelles.

Catalytic transfer hydrogenation of ketones

Complexes **ML^n** (M = Ru, Rh; *n* = 8, 16) were tested as catalysts for water-phase transfer hydrogenation, and acetophenone (**1**) was initially chosen as model substrate. The results of the catalytic tests are listed in Table 2, together with values obtained with the in-situ-prepared ethyl-tailed analogue [(*p*-cymene)RuCl(L^{Et})]Cl (**RuL^{Et}**)[14b] for comparison. The experiments were carried out under nitrogen in Schlenk tubes in degassed water or degassed water/methanol (1:1) solutions.

From comparison of data in Table 2, the effects of the choice of metal and the length of the alkyl tail of the ligand and

Table 2. Transfer hydrogenation of **1** catalyzed by **ML^n**.[a]

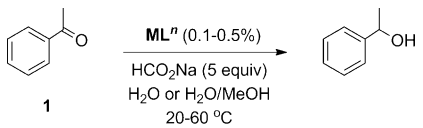

Entry	Catalyst	T [°C]	ω(MeOH) [%]	t [h]	Conver. [%]	TOF [h^{-1}][c]
1[b]	**RuL^{16}**	20	0	7	97	36
2[b]	**RuL^{16}**	20	50	7	40	12
3	**RuL^{16}**	40	0	6	99	330
4	**RuL^{16}**	40	50	6	42	120
5	**RuL^{16}**	60	0	1	98	1500
6	**RuL^{16}**	60	50	1	49	550
7	**RuL^{8}**	60	0	1	51	350
8	**RuL^{8}**	60	50	1	45	520
9	**RuL^{Et}**	60	0	1	11	110
10	**RuL^{Et}**	60	50	1	35	470
11	**RhL^{16}**	20	0	6	88	300
12	**RhL^{16}**	20	50	6	62	160
13	**RhL^{8}**	20	0	6	77	35
14	**RhL^{8}**	20	50	6	55	160

[a] Conditions: **1** (0.25 M), catalyst (0.25 mM), HCOONa (1.25 M), **ML^n**/**1**/HCO$_2$Na 1:1000:5000, water/methanol (4 mL total volume). [b] Conditions: catalyst (1.25 mM), **RuL^{16}**/**1**/HCO$_2$Na 1:200:1000. [c] Initial TOF, defined as (mmol product) (mmol catalyst)$^{-1}$ h^{-1}, measured after 15–30 min.

hence its surface-active properties on the activity can be appreciated at different H$_2$O/MeOH ratios. For **RuL^{16}** (Table 2, entries 1–6) the activity in water is about three times higher than in water/methanol in the temperature range 20–60 °C. The activity of **RuL^{8}** is comparable in water and aqueous methanol (Table 2, entries 7 and 8) and close to that observed for **RuL^{16}** in water/methanol (Table 2, entry 6). In aqueous methanol **RuL^{Et}** is slightly less active (Table 2, entry 10) than the other two ruthenium catalysts, while in neat water (Table 2, entry 9) its activity drops severely and is an order of magnitude lower than that of **RuL^{16}**. Interestingly, this finding is in contrast with earlier reports[14b] that for transfer hydrogenation of benzaldehyde with HCOONa in water at 80 °C, **RuL^{Et}** was significantly more active than **RuL^{8}**.

Generally the rhodium catalysts **RhL^n** are 5–10 times more active at 20 °C (Table 2, entries 11–14) than the corresponding ruthenium analogues, but the largest effect in catalysis was caused by the tail length. At higher temperatures, decomposition of **RhL^n** complexes occurred. This behavior is in line with that recently reported for transfer hydrogenation of **1** in the presence of an Rh TsDPEN complex immobilized on a polymer support.[15c]

Whereas initial turnover frequencies (TOFs) obtained with **ML^n** catalysts in water/methanol do not differ substantially (see Table 2, entries 6, 8, and 10 for M = Ru and entries 12 and 14 for M = Rh) and are almost independent of the nature of ammonium side group, in water a large effect is caused by the length of the alkyl tail at the ammonium group. The long alkyl tail may facilitate phase transfer between substrate and formate or may change the structure of the reaction zone favoring micelle formation.

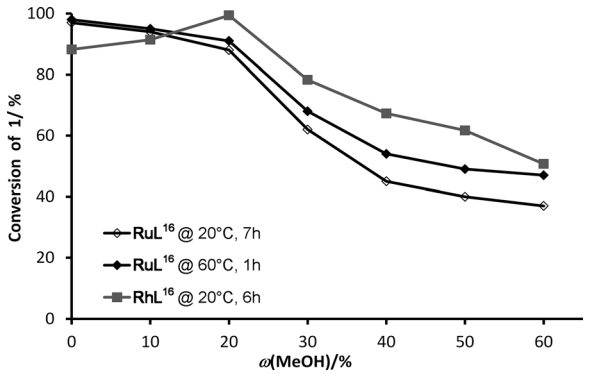

Figure 2. Transfer hydrogenation conversions of **1** catalyzed by **RuL^{16}** and **RhL^{16}** at various water/methanol ratios and temperatures. For conditions, see Table 2.

Increasing the methanol content ω(MeOH) in the reaction mixture decreased the rate of hydrogenation for both **RuL^{16}** and **RhL^{16}** (Figure 2). This effect is most prominent at ω(MeOH) > 30 %. Since **1** dissolves completely in H$_2$O/MeOH mixtures at $\omega \approx 35$ %, surface-active catalyst molecules may become assembled at lower MeOH content and be active at the substrate/water interface. The different behaviors of **RuL^{16}** and **RhL^{16}** at low methanol content ($\omega = 0$–20 %) must be then related to their different organization and hydration in micelles, as already discussed. A detailed study of the reaction profiles in neat water and in water/methanol solutions was then carried out. The results for **RuL^n** and **RhL^n** are treated separately in the following.

Transfer hydrogenation of 1 in the presence of RuL^n

Figure 3 shows the reaction profile for the conversion of **1** with Ru catalysts bearing different alkyl tails at different solvent compositions. Catalysts **RuL^{8}**, **RuL^{16}**, and **RuL^{Et}** perform similarly in 50 % aqueous methanol, showing initial TOFs in the

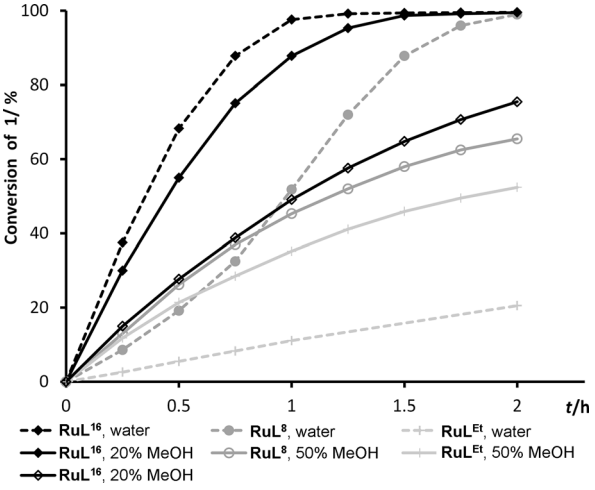

Figure 3. Transfer hydrogenation conversions of **1** catalyzed by **RuL^n** at various water/methanol ratios. Conditions: T = 60 °C, H$_2$O/MeOH (4 mL total volume), HCOONa (1.25 M), **1** (0.25 M), **RuL^n** (0.25 mM), **RuL^n**/**1**/HCO$_2$Na 1:1000:5000.

range 470–550 h^{-1}. The rate was observed to decrease steadily at increasing conversions, in analogy to the common behavior reported for homogeneously catalyzed transfer hydrogenation of ketones.

In neat water, complex **RuL^{Et}** catalyzed the reaction very slowly (TOF = 110 h^{-1}) compared to the surface-active **RuL^{16}** (TOF = 1500 h^{-1}), and both reactions became slower with time. **RuL^{8}** gave a sigmoidal profile, which was rather slow in the beginning (TOF = 350 h^{-1} at 10% conversion) and significantly accelerated at higher conversions (TOF > 800 h^{-1} at 50–70% conversion). The partial solubility of **1** in water (74 mM at 60 °C,[32] lower in the presence of HCO_2Na in solution) limits the hydrogenation rate of **1** catalyzed by **RuL^{Et}**.

It was shown above that the C_{16} alkyl tail allowed **RuL^{16}** to form micelles, with a CMC of about 1.3 mM in neat water. Considering that the CMC of CTAC in 1 M NaCl is about 0.15 mM[33] and that both Cl^- and carboxylate anions have relatively low specific adsorption energy towards micelles formed from $C_nNMe_3^+$,[34] we could estimate the CMC of **RuL^{16}** in 1.25 M HCOONa electrolyte solution to be about 0.1 mM. The concentration of **RuL^{16}** used in transfer hydrogenation (0.25 mM) was above the estimated CMC under these conditions, so during the reaction the catalyst will preferably self-assemble to micelles and will be distributed over the surface of the substrate droplets dispersed in the aqueous phase (Figure 4A). Thus, rate acceleration in this case originated from the ability of **RuL^{16}** to be adsorbed densely on the surface of the liquid organic substrate and to form well-dispersed, highly positively charged droplets with enhanced local concentration of formate ions. In such a micellar system the concentrations of both catalyst and reductant are much higher at the interface of the substrate droplets compared to the bulk solution. A similar situation was recently observed for an iridium catalyst grafted to a linear polymer bearing charged trimethylammonium side-chain groups.[21]

Conversely, **RuL^{8}** aggregates only at high concentrations, and under the reaction conditions applied here should exist as monomers, which are adsorbed on the substrate droplets without forming a dense surface layer, similar to what has been reported for the sparse distribution of SDS molecules over the surface of oil in water.[35] Therefore, **RuL^{8}** is distributed between the bulk aqueous phase and the surface of the substrate droplets (Figure 4B), which gives an overall hydrogenation rate higher than that of **RuL^{Et}**. The sigmoidal shape of the reaction profile and the presence of an induction period for **RuL^{8}** (Figure 3) could be related to increasing formation of the product (1-phenylethanol) and the byproduct sodium carbonate.[36] At increasing concentrations they may improve the adsorption of **RuL^{8}** on the surface of droplets of the ketone. In fact, binegative counterions are known to be adsorbed strongly on the surface of positively charged micelles and thus decrease the CMC of surfactants.[37] Indeed, further rate enhancement was observed on addition of Na_2SO_4 to the reaction mixture (Figure 5). Alcohols are also known to improve surface-active properties of surfactants.[38] This effect was confirmed by adding 1-phenylethanol to the catalytic mixture and observing that the initial rate (TOF = 1300 h^{-1}) strongly increased almost reaching the activity of **RuL^{16}** without any induction period (Figure 5). As expected, no rate enhancement was observed when 1-phenylethanol was added to the **RuL^{Et}**-catalyzed reaction, in which the surface-active effect on the aqueous/organic interface is not present.

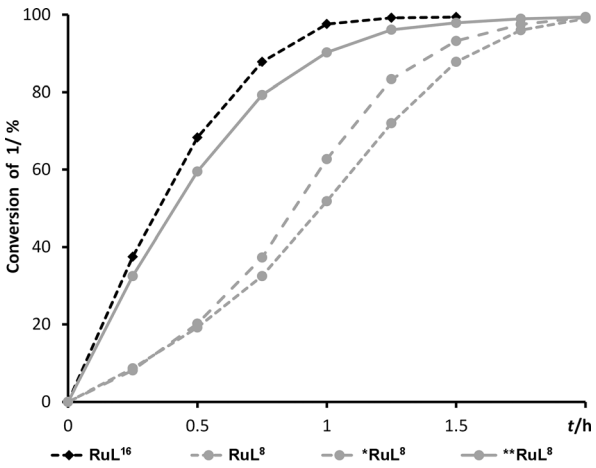

Figure 5. Effect of the addition of salt or product on transfer hydrogenation of **1** catalyzed by **RuL^{n}** complexes in neat water Conditions: T = 60 °C, H_2O (4 mL), HCOONa (1.25 M), **1** (0.25 M), **RuL^{n}** (0.25 mM), **RuL^{n}**/**1**/HCO_2Na 1:1000:5000. * In the presence of Na_2SO_4 (0.125 M). ** In the presence of 1-phenylethanol (0.125 M).

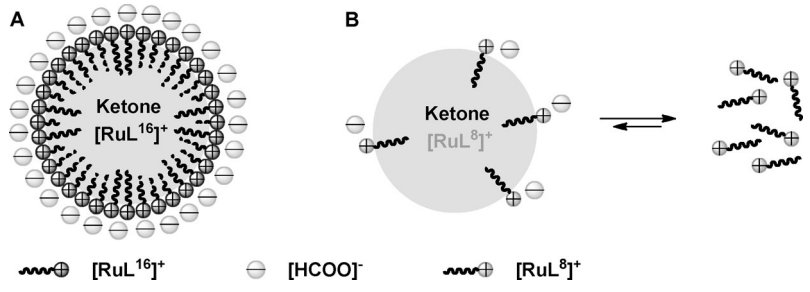

Figure 4. Schematic representation of droplets of **1** in water, stabilized with a dense layer of **RuL^{16}** (A) and sparsely covered with **RuL^{8}** (B).

Transfer hydrogenation of 1 in the presence of RhL^{n}

The reaction profiles of transfer hydrogenation of acetophenone catalyzed by **RhL^{n}** complexes (Figure 6) showed a similar behavior to those of **RuL^{n}** complexes. Again, in 50% aqueous methanol as reaction medium, no significant difference in activity between **RhL^{16}** and **RhL^{8}** was observed, with initial TOFs of

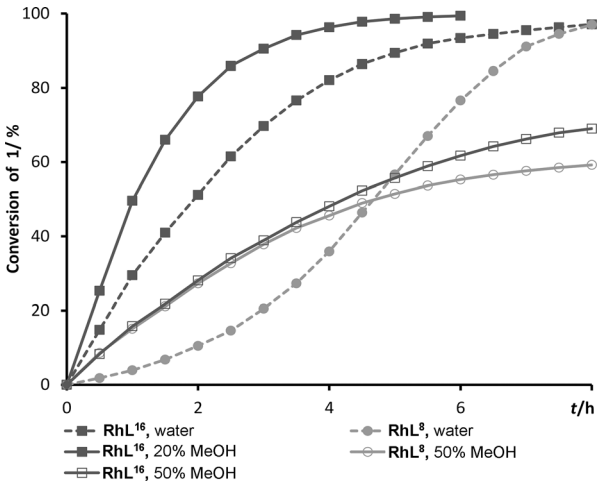

Figure 6. Transfer hydrogenation conversion of **1** catalyzed by **RhL^n** at various water/methanol ratios. Conditions: $T = 20\,^{\circ}C$, H_2O/MeOH (4 mL total volume), HCOONa (1.25 M), **1** (0.25 M), **RhL^n** (0.25 mM), **RhL^n**/**1**/HCO_2Na 1:1000:5000.

160 h^{-1}. In neat water, surface-active **RhL^{16}** performed twice as well (TOF = 300 h^{-1}). Addition of 20% methanol caused an increase in TOF to 500 h^{-1}, in contrast to the behavior observed for **RuL^{16}** (Figure 3).

In the presence of **RhL^8** the reaction profile followed a sigmoidal behavior, with an initial slow rate (TOF = 35 h^{-1}) that increased at higher conversions to reach TOF ≈ 200 h^{-1} at 40–80% conversion. It can be concluded that the two major differences between **RhL^n** and **RuL^n** are the need for small quantities of methanol to gain maximum activity of **RhL^{16}**, and the greater rate enhancement with increasing conversion for **RhL^8** than for **RuL^8**.

As already mentioned, we propose that the reason for such different behavior between Rh and Ru is related to the different hydrophobicities of Cp* versus arene coligands. In **RhL^{16}** the metal center resides entirely in the hydrophobic phase (alkyl tails and acetophenone) at the water/substrate interface (Figure 7), and poor contact with aqueous formate may inhibit fast regeneration of the active rhodium hydride species,[8,10b] which is easier in the presence of MeOH. The slow initial rate found for **RhL^8** can also be attributed to compact folding of the **RhL^8** monomers in water. When enough 1-phenylethanol has accumulated in solution, **RhL^8** is mainly assembled at the substrate droplets and the major contribution to the reaction rate comes from the hydrogenation occurring at the droplet interface.

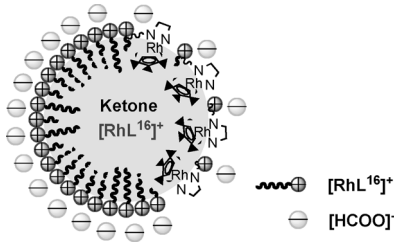

Figure 7. Schematic representation of droplets of **1** in water stabilized by a dense layer of **RhL^{16}** bearing a hydrophobic and poorly hydrated Cp* ligand.

Transfer hydrogenation of hydrophobic ketones 2 and 3 in the presence of ML^n complexes

We were interested in the applicability of the **ML^n** catalysts in the transfer hydrogenation of less water soluble or fully hydrophobic ketones. Poorly water soluble (2.2 mM) butyrophenone (**2**) and hydrophobic dodecanone-2 (**3**) were then chosen as model substrates. The reaction profiles obtained with **RuL^n** are shown in Figure 8.

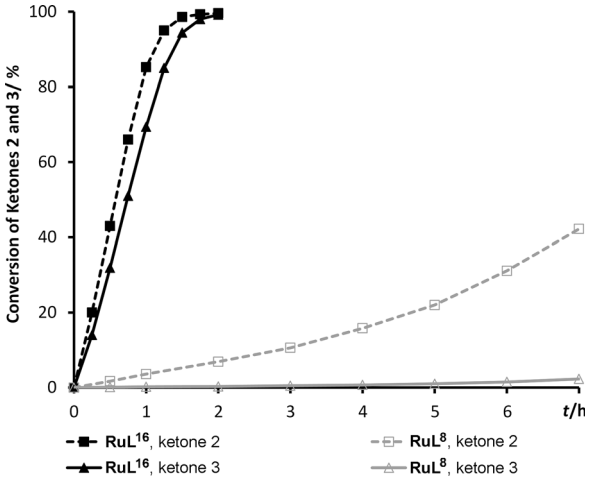

Figure 8. Transfer hydrogenation conversion of **2** and **3** catalyzed by **RuL^n** in neat water. Conditions: $T = 60\,^{\circ}C$, H_2O (4 mL), HCOONa (1.25 M), substrate (0.25 M), **RuL^n** (0.625 mM), Ru/substrate/HCO_2Na 1:400:2000.

For both **2** and **3**, a sharp difference in hydrogenation rates in water between the catalysts **RuL^8** and **RuL^{16}** was observed. In the case of **RuL^{16}**, the initial TOFs were 350 and 280 h^{-1} for **2** and **3**, respectively, which are only 4–5 times lower than for **1** (TOF = 1500 h^{-1}). Conversely, the activity of **RuL^8** in water dropped severely when hydrophobic ketones **2** (initial TOF = 14 h^{-1}) and **3** (initial TOF = 0.8 h^{-1}) were used instead of **1**. At longer reaction times, however, the same acceleration effect previously described for **1** was observed. Again, the low surface activity of **RuL^8**, which did not micellize the hydrophobic ketones efficiently at the beginning of the reaction, is mitigated by prolonged stirring and accumulation of the alcohol product with time and allows hydrogenation of hydrophobic ketones **2** and **3**, albeit with low efficiency. When **RhL^n** complexes were tested in neat water under the same conditions applied for hydrogenation of **1**, very low activities in hydrogenation of the hydrophobic ketones **2** and **3** were observed, with TOF ≤ 10 and TOF ≪ 1 for **RhL^{16}** and **RhL^8**, respectively, as expected for these less surface active catalysts.

Conclusion

In our search for efficient micellar catalysts for transfer hydrogenation of ketones we have developed a novel one-pot synthetic route to Ts-EN ligands modified with trialkyl ammonium side groups **HL^n** and obtained the surface active Noyori-type complexes [(*p*-cymene)RuCl(**L^n**)] and [Cp*RhCl(**L^n**)]. The complexes with C_{16} alkyl tails **ML^{16}** form micelles and are densely adsorbed at the water/substrate interface, where they strongly enhance the rate of catalytic transfer hydrogenation of ketones with formate in water compared to complexes with shorter alkyl chains. Our straightforward approach gives a self-organized catalyst system directly in the reaction mixture. Such an approach is applicable also for hydrophobic ketones, for which the use of the Ru-based micellar catalysts boosts the hydrogenation rates by as much as two orders of magnitude compared to nonmicellar ones. The different abilities of the ligands to self-assemble and form micelles was rationalized by using a combination of methods including DOSY NMR and surface-tension measurements, and correlated to the observed reaction profiles. Ligand modification to give chiral surface-active catalysts for efficient ATH of hydrophobic ketones in water are in progress.

Experimental Section

General procedures

All manipulations were carried out by using standard Schlenk techniques under an atmosphere of dry argon or nitrogen. Solvents were purified by standard methods and distilled prior to use. [{(*p*-cymene)RuCl$_2$}$_2$][39] and [{Cp*RhCl$_2$}$_2$][40] were prepared according to described methods. Other reagents were purchased from commercial sources in the highest available purity and used as received. ^{1}H and ^{13}C{^{1}H} NMR spectra were recorded at room temperature (25 °C) on a Bruker ARX-400 spectrometer operating at frequencies of 400 and 100 MHz, respectively, and referenced to the residual proton signals of the deuterated solvent. Elemental analyses were performed in the Laboratory of Microanalysis at INEOS RAS either manually (for Ru samples) or on a Carlo Erba 1106 CHN analyzer. Electrospray mass spectrometry (ESI-MS) was carried out at the University of Florence, Italy, on a LCQ Orbitrap mass spectrometer (ThermoFischer, San Jose, CA, USA) equipped with a conventional ESI source by direct injection of the sample solution and are reported in the form *m/z* (intensity relative to base = 100). GC analyses were performed on a Shimadzu 2010 gas chromatograph equipped with a flame ionization detector and a VF-WAXms capillary column (30 m, 0.25 mm i.d., 0.25 μm film thickness).

General procedure for synthesis of [HL^n]Cl·HCl

A solution of *N*-Boc-ethylenediamine (1.00 equiv) and trialkyl amine (1.05 equiv) in dichloromethane (40 mL) was added dropwise to a solution of (4-bromomethyl)benzenesulfonyl chloride (5.00 mmol, 1.00 equiv) in dichloromethane (50 mL) cooled to 0 °C with an ice bath over 0.5 h. The resulting solution was stirred for an additional 0.5 h followed by addition of neat trialkyl amine (1.20 equiv). The reaction mixture was allowed to warm to room temperature and stirred for 4 h. The final clear solution was concentrated to dryness; the residue was washed with diethyl ether (3×50 mL) to remove unconverted amine. The insoluble pale beige powder was dissolved in methanol (30 mL) and treated with an aqueous solution of $KHCO_3$ (1 g in 10 mL H_2O) for 4 h. The suspension was concentrated to dryness, washed with diethyl ether (3×50 mL) and dried. Finally the solid was quenched with concentrated HCl (15–20 mL of 12 M aqueous solution); after all gas had evolved (ca. 15 min), the resulting solution was concentrated to dryness. The treatment with concentrated aqueous HCl was repeated one more time. After solvent evaporation the glassy solid was dissolved in ethanol (50 mL), the precipitate was filtered off, and the filtrate was evaporated to dryness to give off-white or pale beige glassy foam.

[HL^8]Cl·HCl: (4-Bromomethyl)benzenesulfonyl chloride (1.35 g, 5.00 mmol), *N*-Boc-ethylenediamine (800 μL, 5.00 mmol), and *N,N*-dimethyloctylamine (2.31 mL, 11.25 mmol) afforded 2.10 g (95%) of the product. ^{1}H NMR (CD_3OD): $\delta = 8.02$ (d, $^3J = 8.4$ Hz, 2H; C_6H_4), 7.83 (d, $^3J = 8.4$ Hz, 2H; C_6H_4), 4.66 (s, 2H; CH_2Ar), 3.38 (m, 2H; Me_2NCH_2), 3.15 (t, $^3J = 5.6$ Hz, 2H; NCH_2CH_2N), 3.07 (t, $^3J = 5.6$ Hz, 2H; NCH_2CH_2N), 3.07 (s, 6H; NMe_2), 1.89 (m, 2H; $Me_2NCH_2CH_2$), 1.26–1.44 (m, 10H; 5CH_2), 0.90 ppm (t, $^3J = 6.8$ Hz, 3H; CH_3); ^{13}C{^{1}H} NMR (CD_3OD): $\delta = 141.9$ (*i*-*C*(C_6H_4)), 133.9 (*C*H(C_6H_4)), 132.3 (*i*-*C*(C_6H_4)), 127.5 (*C*H(C_6H_4)), 66.2 (Me_2NCH_2), 65.0 (CH_2NMe_2), 49.2 (NMe_2), 40.2 (NCH_2CH_2N), 39.3 (NCH_2CH_2N), 31.5 (CH_2), 28.8 (2CH_2), 26.0 (CH_2), 22.3 (2CH_2), 13.0 ppm (CH_3); elemental analysis calcd (%) for $C_{19}H_{37}Cl_2N_3O_2S$: C 51.57, H 8.43, N 9.50; found: C 51.16, H 8.24, N 9.27.

[HL^{16}]Cl·HCl: (4-Bromomethyl)benzenesulfonyl chloride (1.36 g, 5.05 mmol), *N*-Boc-ethylenediamine (820 μL, 5.12 mmol), and *N,N*-dimethylhexadecylamine (3.84 mL, 11.36 mmol) afforded 2.60 g (93%) of the product. ^{1}H NMR (CD_3OD): $\delta = 8.04$ (d, $^3J = 8.4$ Hz, 2H; C_6H_4), 7.84 (d, $^3J = 8.4$ Hz, 2H; C_6H_4), 4.66 (s, 2H; CH_2Ar), 3.39 (m, 2H; Me_2NCH_2), 3.16 (t, $^3J = 5.6$ Hz, 2H; NCH_2CH_2N), 3.09 (t, $^3J = 5.6$ Hz, 2H; NCH_2CH_2N), 3.08 (s, 6H; NMe_2), 1.91 (m, 2H; $Me_2NCH_2CH_2$), 1.26–1.45 (m, 26H; 13CH_2), 0.90 ppm (t, $^3J = 6.8$ Hz, 3H; CH_3); ^{13}C{^{1}H} NMR (CD_3OD): $\delta = 142.5$ (*i*-*C*(C_6H_4)), 133.8 (*C*H(C_6H_4)), 132.1 (*i*-*C*(C_6H_4)), 127.4 (*C*H(C_6H_4)), 66.2 (Me_2NCH_2), 65.0 (CH_2NMe_2), 49.2 (NMe_2), 43.3 (NCH_2CH_2N), 40.3 (NCH_2CH_2N), 31.7 (CH_2), 29.4 (6CH_2), 29.3 (CH_2), 29.2 (CH_2), 29.1 (CH_2), 28.9 (CH_2), 26.1 (CH_2), 22.3 (2CH_2), 13.1 ppm (CH_3); elemental analysis calcd (%) for $C_{27}H_{53}Cl_2N_3O_2S{\cdot}2H_2O$: C 54.90, H 9.73, N 7.11; found: C 54.93, H 9.71, N 6.77.

[HL^{Et}]Cl·HCl: (4-Bromomethyl)benzenesulfonyl chloride (2.10 g, 7.80 mmol), *N*-Boc-ethylenediamine (1250 μL, 7.80 mmol) and triethylamine (2.50 mL, 17.9 mmol) afforded 2.92 g (97%) of the product. ^{1}H NMR (CD_3OD): $\delta = 8.01$ (d, $^3J = 8.4$ Hz, 2H; C_6H_4), 7.81 (d, $^3J = 8.4$ Hz, 2H; C_6H_4), 4.61 (s, 2H; CH_2Ar), 3.31 (q, $^3J = 7.6$ Hz, 6H; NCH_2Me), 3.15 (t, $^3J = 5.8$ Hz, 2H; NCH_2CH_2N), 3.07 (t, $^3J = 5.8$ Hz, 2H; NCH_2CH_2N), 1.43 ppm (t, $^3J = 7.6$ Hz, 9H; CH_3); ^{13}C{^{1}H} NMR (CD_3OD): $\delta = 141.7$ (*i*-*C*(C_6H_4)), 133.5 (*C*H(C_6H_4)), 132.2 (*i*-*C*(C_6H_4)), 127.6 (*C*H(C_6H_4)), 59.0 (Aryl-CH_2N), 52.7 (NCH_2Me), 40.0 (NCH_2CH_2N), 39.3 (NCH_2CH_2N), 6.8 ppm (CH_3).

General procedure for synthesis of [(*p*-cymene)Ru(L^n)Cl]Cl (RuL^8, RuL^{16}) and [Cp*Rh(L^n)Cl]Cl (RhL^8, RhL^{16})

A solution of $KHCO_3$ (100 mg, 1.0 mmol) and NaCl (300 mg, 5.1 mmol) in H_2O (2 mL) was added to a solution of [{(*p*-cymene)RuCl$_2$}$_2$] or [{Cp*RhCl$_2$}$_2$] (0.15 mmol) and ligand salt **[H$_2$L^n]Cl$_2$** (0.31 mmol) in dichloromethane (20 mL); the biphasic mixture was vigorously stirred overnight. The water/organic layers were allowed to separate for 2 h. The lightly colored upper aqueous layer was discarded; the organic layer was dried over Na_2SO_4 and filtered, and the solvent was removed in vacuo to afford the product as a yellow or orange powder.

RuL[8]: [{(*p*-cymene)$RuCl_2$}$_2$] (92 mg, 0.15 mmol) and **[H_2L^8]Cl_2** (137 mg, 0.31 mmol) afforded 170 mg (84%) of [(*p*-cymene)Ru(L^8)Cl]Cl as a yellow-orange powder. ^{1}H NMR (CD_2Cl_2): δ = 7.78 (d, ^3J = 8.4 Hz, 2H; C_6H_4), 7.51 (d, ^3J = 8.4 Hz, 2H; C_6H_4), 7.13 (br d, $J \approx 10$ Hz, 1H; NH), 5.90 (d, ^3J = 6.0 Hz, 1H; C_6H_4(cymene)), 5.76 (d, ^3J = 5.6 Hz, 1H; C_6H_4(cymene)), 5.69 (d, ^3J = 5.6 Hz, 1H; C_6H_4-(cymene)), 5.43 (d, ^3J = 6.0 Hz, 1H; C_6H_4(cymene)), 4.83 (d, ^2J = 12.4 Hz, 1H; C*H*HAr), 4.78 (d, ^2J = 12.4 Hz, 1H; C*H*HAr), 3.40 (m, 2H; Me_2NCH_2), 3.11 (s, 3H; NMe_2), 3.10 (s, 3H; NMe_2), 2.94 (br m, 1H; NCH*H*CH_2N), 2.93 (sept, ^3J = 6.8 Hz, 1H; Me_2CH(cymene)), 2.65 (br m, 2H; NCH_2CH_2N), 2.20 (br m, 1H; NC*H*HCH_2N), 2.11 (s, 3H; Me-(cymene)), 2.02 (br t, $J \approx 10$ Hz, 1H; NH), 1.78 (br m, 2H; $Me_2NCH_2CH_2$), 1.18–1.40 (m, 10H; 5CH_2), 1.24 (d, ^3J = 6.8 Hz, 3H; Me_2CH(cymene)), 1.23 (d, ^3J = 6.8 Hz, 3H; Me_2CH(cymene)), 0.89 ppm (t, ^3J = 6.8 Hz, 3H; CH_3); ^{13}C{^{1}H} NMR (CD_2Cl_2): δ = 145.9 (*i*-$C(C_6H_4)$), 132.5 ($CH(C_6H_4)$), 128.3 (*i*-$C(C_6H_4)$), 127.6 ($CH(C_6H_4)$), 101.4 (*i*-*C*(cymene)), 97.0 (*i*-*C*(cymene)), 82.3 (*C*H(cymene)), 82.2 (*C*H-(cymene)), 80.8 (*C*H(cymene)), 80.4 (*C*H(cymene)), 67.1 (Me_2NCH_2), 64.4 (CH_2NMe_2), 49.8 (NMe_2), 49.7 (NMe_2), 48.9 (NCH_2CH_2N), 47.0 (NCH_2CH_2N), 31.7 (CH_2), 30.4 (Me_2CH(cymene)), 29.2 (CH_2), 29.1 (CH_2), 26.3 (CH_2), 23.0 (Me_2CH(cymene)), 22.9 (CH_2), 22.6 (CH_2), 21.6 (Me_2CH(cymene)), 18.6 (*Me*(cymene)), 13.9 ppm (CH_3); ESI-MS (MeOH): *m/z* (%): 640.23 (55) [M^+], 604.25 (45) [M^+−HCl]; elemental analysis calcd (%) for $C_{29}H_{49}Cl_2N_3O_2RuS$: C 51.54, H 7.31; found: C 51.67, H 7.58.

RuL[16]: [{(*p*-cymene)$RuCl_2$}$_2$] (92 mg, 0.15 mmol) and **[H_2L^{16}]Cl_2** (172 mg, 0.31 mmol) afforded 210 mg (89%) of [(*p*-cymene)Ru(**L^{16}**)Cl]Cl as a yellow powder. ^{1}H NMR (CD_2Cl_2): δ = 7.78 (d, ^3J = 8.4 Hz, 2H; C_6H_4), 7.51 (d, ^3J = 8.4 Hz, 2H; C_6H_4), 7.11 (br d, $J \approx 10$ Hz, 1H; NH), 5.89 (d, ^3J = 6.0 Hz, 1H; C_6H_4(cymene)), 5.76 (d, ^3J = 5.6 Hz, 1H; C_6H_4(cymene)), 5.68 (d, ^3J = 5.6 Hz, 1H; C_6H_4-(cymene)), 5.42 (d, ^3J = 6.0 Hz, 1H; C_6H_4(cymene)), 4.82 (d, ^2J = 12.4 Hz, 1H; C*H*HAr), 4.77 (d, ^2J = 12.4 Hz, 1H; C*H*HAr), 3.39 (m, 2H; Me_2NCH_2), 3.11 (s, 3H; NMe_2), 3.10 (s, 3H; NMe_2), 2.94 (br m, 1H; NCH*H*CH_2N), 2.92 (sept, ^3J = 6.8 Hz, 1H; Me_2CH(cymene)), 2.65 (br m, 2H; NCH_2CH_2N), 2.20 (br m, 1H; NC*H*HCH_2N), 2.10 (s, 3H; Me-(cymene)), 2.01 (br t, $J \approx 10$ Hz, 1H; NH), 1.80 (br m, 2H; $Me_2NCH_2CH_2$), 1.18–1.40 (m, 26H; 13CH_2), 1.24 (d, ^3J = 6.8 Hz, 3H; Me_2CH(cymene)), 1.23 (d, ^3J = 6.8 Hz, 3H; Me_2CH(cymene)), 0.88 ppm (t, ^3J = 6.8 Hz, 3H; CH_3); ^{13}C{^{1}H} NMR (CD_2Cl_2): δ = 145.6 (*i*-$C(C_6H_4)$), 132.6 ($CH(C_6H_4)$), 128.6 (*i*-$C(C_6H_4)$), 127.6 ($CH(C_6H_4)$), 101.9 (*i*-*C*(cymene)), 96.5 (*i*-*C*(cymene)), 82.5 (*C*H(cymene)), 81.9 (*C*H-(cymene)), 81.1 (*C*H(cymene)), 80.5 (*C*H(cymene)), 67.2 (Me_2NCH_2), 64.3 (CH_2NMe_2), 49.5 (NMe_2), 49.3 (NMe_2), 49.0 (NCH_2CH_2N), 47.0 (NCH_2CH_2N), 31.9 (CH_2), 30.4 (Me_2CH(cymene)), 29.7 (5CH_2), 29.5 (2CH_2), 29.4 (2CH_2), 26.4 (CH_2), 23.2 (Me_2CH(cymene)), 23.0 (CH_2), 22.7 (2CH_2), 21.9 (Me_2CH(cymene)), 18.7 (*Me*(cymene)), 14.1 ppm (CH_3); ESI-MS (MeOH): *m/z* (%): 752.35 (55) [M^+], 716.38 (45) [M^+−HCl]; elemental analysis calcd (%) for $C_{37}H_{65}Cl_2N_3O_2RuS$: C 56.40, H 8.31; found: C 56.44, H 8.35.

RhL[8]: [{Cp*$RhCl_2$}$_2$] (92 mg, 0.15 mmol) and **[H_2L^8]Cl_2** (137 mg, 0.31 mmol) afforded 180 mg (88%) of [Cp*Rh(L^8)Cl]Cl as an orange powder. ^{1}H NMR (CD_3OD): δ = 8.00 (d, ^3J = 8.4 Hz, 2H; C_6H_4), 7.55 (d, ^3J = 8.4 Hz, 2H; C_6H_4), 4.54 (s, 2H; CH_2Ar), 3.30 (m, 2H; Me_2NCH_2), 3.03 (s, 6H; NMe_2), 2.65 (t, ^3J = 5.2 Hz, 2H; NCH_2CH_2N), 2.49 (t, ^3J = 5.2 Hz, 2H; NCH_2CH_2N), 1.88 (m, 2H; $Me_2NCH_2CH_2$), 1.75 (s, 15H; C_5Me_5), 1.28–1.45 (m, 10H; 5CH_2), 0.92 ppm (t, ^3J = 6.8 Hz, 3H; CH_3); ^{13}C{^{1}H} NMR (CD_3OD): δ = 145.7 (*i*-$C(C_6H_4)$), 132.4 ($CH(C_6H_4)$), 129.4 (*i*-$C(C_6H_4)$), 128.2 ($CH(C_6H_4)$), 94.2 (d, ^2J(Rh,C) = 8.5 Hz, C_5Me_5), 66.8 (Me_2NCH_2), 64.4 (CH_2NMe_2), 49.7 (NMe_2), 49.1 (NCH_2CH_2N), 45.6 (NCH_2CH_2N), 31.5 (CH_2), 28.8 (2CH_2), 26.0 (CH_2), 22.3 (2CH_2), 13.0 (CH_3), 8.1 ppm (C_5Me_5); ESI-MS (MeOH): *m/z* (%): 642.25 (93) [M^+], 606.26 (7) [M^+−HCl]; elemental analysis calcd (%) for $C_{29}H_{50}Cl_2N_3O_2RhS{\cdot}2H_2O$: C 48.74, H 7.62, N 5.88; found: C 48.64, H 7.48, N 5.81.

RhL[16]: [{Cp*$RhCl_2$}$_2$] (92 mg, 0.15 mmol) and **[H_2L^{16}]Cl_2** (172 mg, 0.31 mmol) afforded 220 mg (93%) of [Cp*Rh(L^{16})Cl]Cl as an orange powder. ^{1}H NMR (CD_3OD): δ = 7.99 (d, ^3J = 8.4 Hz, 2H; C_6H_4), 7.55 (d, ^3J = 8.4 Hz, 2H; C_6H_4), 4.54 (s, 2H; CH_2Ar), 3.29 (m, 2H; Me_2NCH_2), 3.03 (s, 6H; NMe_2), 2.66 (t, ^3J = 5.6 Hz, 2H; NCH_2CH_2N), 2.49 (t, ^3J = 5.6 Hz, 2H; NCH_2CH_2N), 1.88 (m, 2H; $Me_2NCH_2CH_2$), 1.76 (s, 15H; C_5Me_5), 1.26–1.46 (m, 26H; 13CH_2), 0.90 ppm (t, ^3J = 6.8 Hz, 3H; CH_3); ^{13}C{^{1}H} NMR (CD_3OD): δ = 145.7 (*i*-$C(C_6H_4)$), 132.3 ($CH(C_6H_4)$), 129.4 (*i*-$C(C_6H_4)$), 128.2 ($CH(C_6H_4)$), 94.3 (d, ^2J(Rh,C) = 8.5 Hz, C_5Me_5), 66.8 (Me_2NCH_2), 64.4 (CH_2NMe_2), 49.7 (NMe_2), 49.1 (NCH_2CH_2N), 45.6 (NCH_2CH_2N), 31.7 (CH_2), 29.4 (5CH_2), 29.3 (CH_2), 29.2 (CH_2), 29.1 (CH_2), 29.0 (CH_2), 28.8 (CH_2), 26.0 (CH_2), 22.3 (2CH_2), 13.0 (CH_3), 8.2 ppm (C_5Me_5); ESI-MS (MeOH): *m/z* (%): 754.37 (95) [M^+], 718.39 (5) [M^+−HCl]; elemental analysis calcd (%) for $C_{37}H_{66}Cl_2N_3O_2RhS$: C 56.19, H 8.41, N 5.31; found: C 56.39, H 8.45, N 5.19.

Transfer hydrogenation tests

The reactions were carried out in Schlenk tubes under an inert atmosphere in degassed solvents. Typically the solution of HCO_2Na in water or water/methanol of desired concentration was prepared directly in the reaction tube. The temperature was set and a fresh 5 mM solution of the precatalyst in degassed water was added to reach a total volume of 4 mL. Finally the liquid substrate was directly added by syringe to the reaction mixture under vigorous stirring. An aliquot of the reaction mixture (0.05 mL) was taken by syringe and diluted with methanol (0.4 mL) or extracted with ethyl acetate (0.8 mL) before being analyzed by GC. The aliquots in methanol were usually passed through a plug of silica before injection to remove traces of metal and salts. Each test was repeated at least twice to check for reproducibility.

DOSY measurements

DOSY experiments were performed on a Bruker Avance 600 spectrometer at 25 °C by using the DOSY-ONESHOT[41] pulse sequence. The following experimental parameters of the pulse sequence were used: diffusion time 0.4 s, gradient pulse duration 2.5 ms, unbalancing factor alpha 2.0, relaxation delay 5.0 s. Signal attenuation was achieved by increasing the gradient strength from 5 to 80% as defined by the pulse sequence in 16 steps with 16 scans each and maximum gradient strength of 0.27 T m^{-1}. The rows of the pseudo-2D diffusion dataset were phased and baseline-corrected. The pseudo-2D DOSY spectra were constructed by using standard fitting procedure of the Bruker Topspin 2.1 software. The true diffusion coefficients were determined by using the T_1/T_2 analysis module of the Bruker Topspin 2.1 software. Viscosities of the solution were obtained by comparing the measured diffusion coefficients of the residual proton-containing solvents with the known values (1.902×10^{-9} m^2 s^{-1} for HDO in D_2O[42] and 2.41×10^{-9} m^2 s^{-1} for MeOH in CD_3OD[43]). The hydrodynamic radii and volumes were calculated from viscosity-corrected diffusion coefficients via the Stokes–Einstein relation.

Determination of CMC

Surface tensions γ at the air/solution interface were measured by the Wilhelmy plate method (KSV Sigma tensiometer, Finland) at 25 ± 0.5 °C. Solutions of **RuL[16]** and **RhL[16]** were prepared in the concentration ranges of 0.05–5 mM and 0.05–1.5 mM, respectively, in deionized water (16 MΩ resistivity) and were equilibrated at room temperature for 48 h. The platinum plate was cleaned and heated

with a gas burner before each measurement. The γ value was measured after allowing about 20 min for equilibration. The experiments were repeated twice to check for reproducibility, and the mean values were used for data treatment. The γ values were accurate within ± 0.1 mN m^{-1}. The results were graphically processed to determine the CMC.

Acknowledgements

This research was fully supported by a Marie Curie International Incoming Fellowships within the 7th European Community Framework Programme (grant no. PIIF-GA-2009–236423, MODUCAT).

Keywords: hydrogenation · micellar catalysis · rhodium · ruthenium · water-soluble ligands

[1] a) S. Hashiguchi, A. Fujii, J. Takehara, T. Ikariya, R. Noyori, *J. Am. Chem. Soc.* **1995**, *117*, 7562 – 7563; b) R. Noyori, S. Hashiguchi, *Acc. Chem. Res.* **1997**, *30*, 97 – 102.

[2] a) K. Mashima, T. Abe, K. Tani, *Chem. Lett.* **1998**, 1201 – 1202; b) K. Murata, T. Ikariya, *J. Org. Chem.* **1999**, *64*, 2186 – 2187.

[3] X. Wu, J. Liu, X. Li, A. Zanotti-Gerosa, F. Hancock, D. Vinci, J. Ruan, J. Xiao, *Angew. Chem.* **2006**, *118*, 6870 – 6874; *Angew. Chem. Int. Ed.* **2006**, *45*, 6718 – 6722.

[4] a) N. Uematsu, A. Fujii, S. Hashiguchi, T. Ikariya, R. Noyori, *J. Am. Chem. Soc.* **1996**, *118*, 4916 – 4917; b) J. Wu, F. Wang, Y. Ma, X. Cui, L. Cun, J. Zhu, J. Deng, B. Yu, *Chem. Commun.* **2006**, 1766 – 1768.

[5] P. Peach, D. J. Cross, J. A. Kenny, I. Mann, I. Houson, L. Campbell, T. Walsgrove, M. Wills, *Tetrahedron* **2006**, *62*, 1864 – 1876.

[6] K. Matsumura, S. Hashiguchi, T. Ikariya, R. Noyori, *J. Am. Chem. Soc.* **1997**, *119*, 8738 – 8739.

[7] a) Y. Ma, H. Liu, L. Chen, X. Cui, J. Zhu, J. Deng, *Org. lett.* **2003**, *5*, 2103 – 2106; b) F. Wang, H. Liu, L. Cun, J. Zhu, J. Deng, Y. Jiang, *J. Org. Chem.* **2005**, *70*, 9424 – 9429.

[8] X. Li, L. Li, Y. Tang, L. Zhong, L. Cun, J. Zhu, J. Liao, J. Deng, *J. Org. Chem.* **2010**, *75*, 2981 – 2988.

[9] H. Y. Rhyoo, H. J. Park, Y. K. Chung, *Chem. Commun.* **2001**, 2064 – 2065.

[10] a) X. F. Wu, J. L. Xiao, *Chem. Commun.* **2007**, 2449 – 2466; b) W. Xiaofeng, W. Chao, X. Jianliang, *Platinum Met. Rev.* **2010**, *54*, 3 – 19; c) C. Wang, X. Wu, J. Xiao, *Chem. Asian J.* **2008**, *3*, 1750 – 1770.

[11] T. Thorpe, J. Blacker, S. M. Brown, C. Bubert, J. Crosby, S. Fitzjohn, J. P. Muxworthy, J. M. J. Williams, *Tetrahedron Lett.* **2001**, *42*, 4041 – 4043.

[12] a) X. G. Li, X. F. Wu, W. P. Chen, F. E. Hancock, F. King, J. L. Xiao, *Org. Lett.* **2004**, *6*, 3321 – 3324; b) X. G. Li, W. P. Chen, W. Hems, F. King, J. L. Xiao, *Tetrahedron Lett.* **2004**, *45*, 951 – 953; c) Z. Zhongqiang, S. Yong, *React. Kinet. Mech. Catal.* **2010**, *99*, 391 – 396.

[13] a) N. A. Cortez, G. Aguirre, M. Parra-Hake, R. Somanathan, *Tetrahedron Lett.* **2007**, *48*, 4335 – 4338; b) Z. Zhongqiang, S. Yong, *Catal. Commun.* **2009**, *10*, 1685 – 1688; c) Z. Zhou, Q. Ma, Y. Sun, A. Zhang, L. Li, *Heteroat. Chem.* **2010**, *21*, 505 – 514.

[14] a) Z. Zhou, Q. Ma, A. Zhang, L. Wu, *Appl. Organomet. Chem.* **2011**, *25*, 856 – 861; b) H. Huo, Z. Zhou, A. Zhang, L. Wu, *Res. Chem. Intermed.* **2012**, *38*, 261 – 268.

[15] a) A. Yukihiro, C. Atsuko, H. Naoki, I. Shinichi, *Adv. Synth. Catal.* **2008**, *350*, 2295 – 2304; b) H. Naoki, N. Akihiro, I. Shinichi, *J. Polym. Sci. Part A* **2010**, *48*, 3340 – 3349; c) D. Jonas, S. Uwe, K. Juliane, H. Rainer, S. Reinhard, *Adv. Synth. Catal.* **2011**, *353*, 1335 – 1344.

[16] M. Babin, R. Clement, J. Gagnon, F.-G. Fontaine, *New J. Chem.* **2012**, *36*, 1548 – 1551.

[17] X. F. Wu, X. G. Li, W. Hems, F. King, J. L. Xiao, *Org. Biomol. Chem.* **2004**, *2*, 1818 – 1821.

[18] K. Ahlford, J. Lind, L. Mäler, H. Adolfsson, *Green Chem.* **2008**, *10*, 832 – 835.

[19] H. Y. Rhyoo, H. J. Park, W. H. Suh, Y. K. Chung, *Tetrahedron Lett.* **2002**, *43*, 269 – 272.

[20] W. Weiwei, L. Zhiming, M. Wenbo, S. Ling, W. Quanrui, *Catal. Commun.* **2010**, *11*, 480 – 483.

[21] J. Li, Y. Zhang, D. Han, G. Jia, J. Gao, L. Zhong, C. Li, *Green Chem.* **2008**, *10*, 608 – 611.

[22] J. Li, Yu. Tang, Q. Wang, X. Li, L. Cun, X. Zhang, J. Zhu, L. Li, J. Deng, *J. Am. Chem. Soc.* **2012**, *134*, 18522 – 18525.

[23] G. O. Nevstad, J. Songstad, *Acta Chem. Scand. B.* **1984**, *38*, 469 – 477.

[24] C. S. Johnson Jr., *Prog. Nucl. Magn. Reson. Spectrosc.* **1999**, *34*, 203 – 256.

[25] Y. Cohen, L. Avram, L. Frish, *Angew. Chem.* **2005**, *117*, 524 – 560; *Angew. Chem. Int. Ed.* **2005**, *44*, 520 – 554.

[26] Y. Bakkour, V. Darcos, S. Li, J. Coudane, *Polym. Chem.* **2012**, *3*, 2006 – 2010.

[27] B. Naskar, A. Dan, S. Ghosh, V. K. Aswal, S. P. Moulik, *J. Mol. Liq.* **2012**, *170*, 1 – 10.

[28] The PCTs observed for both complexes are most likely due to impurities present in 95% grade *N*,*N*-dimethylhexadecylamine used in their synthesis, which according to Sigma-Aldrich contains as contaminants C_{15}–C_{19} dimethyl alkyl amines.

[29] J. Mata, D. Varade, P. Bahadur, *Thermochim. Acta* **2005**, *428*, 147 – 155.

[30] J. B. Hayter, J. Penfold, *Prog. Colloid Polym. Sci.* **1983**, *261*, 1022 – 1030.

[31] J. M. Del Rio, G. Prieto, F. Sarmiento, V. Mosquera, *Langmuir* **1995**, *11*, 1511 – 1514.

[32] R. M. Stephenson, *J. Chem. Eng. Data* **1992**, *37*, 80 – 95.

[33] T. Imae, S. Ikeda, *Colloid Polym. Sci.* **1987**, *265*, 1090 – 1098.

[34] I. B. Ivanov, R. I. Slavchov, E. S. Basheva, D. Sidzhakova, S. I. Karakashev, *Adv. Colloid Interface Sci.* **2011**, *168*, 93 – 104.

[35] H. B. de Aguiar, M. L. Strader, A. G. F. de Beer, S. Roke, *J. Phys. Chem. B* **2011**, *115*, 2970 – 2978.

[36] X. Wu, J. Liu, D. Di Tommaso, J. Iggo, C. Catlow, J. Bacsa, J. Xiao, *Chem. Eur. J.* **2008**, *14*, 7699 – 7715.

[37] a) B. W. Ninham, V. Yaminsky, *Langmuir* **1997**, *13*, 2097 – 2108; b) E. Feitosa, M. R. S. Brazolin, R. Naal, M. Del Lama, J. R. Lopes, W. Loh, M. Vasilescu, *J. Colloid Interface Sci.* **2006**, *299*, 883 – 889.

[38] a) R. Zana, *Adv. Colloid Interface Sci.* **1995**, *57*, 1 – 64; b) F. Lima, I. M. Cuccovia, D. Horinek, L. Q. Amaral, K. A. Riske, S. Schreier, R. K. Salinas, E. L. Bastos, P. A. R. Pires, J. C. Bozelli, D. C. Favaro, A. C. B. Rodrigues, L. G. Dias, O. A. El Seoud, H. Chaimovich, *Langmuir* **2013**, *29*, 4193 – 4203.

[39] S. B. Jensen, S. J. Rodger, M. D. Spicer, *J. Organomet. Chem.* **1998**, *556*, 151 – 158.

[40] C. White, A. Yates, P. M. Maitlis, *Inorg. Synth.* **1992**, *29*, 228 – 234.

[41] M. D. Pelta, G. A. Morris, M. J. Stchedroff, S. J. Hammond, *Magn. Reson. Chem.* **2002**, *40*, S147 – S152.

[42] M. Holz, H. Weingartner, *J. Magn. Reson.* **1991**, *92*, 115 – 125.

[43] M. Holz, X. A. Mao, D. Seiferling, A. Sacco, *J. Chem. Phys.* **1996**, *104*, 669 – 679.

Received: May 2, 2013
Revised: October 8, 2013
Published online on December 12, 2013

